

# Economic Opportunities for Industrial Systems from Frequency Regulation Markets

Alexander W. Dowling and Victor M. Zavala\*

Department of Chemical and Biological Engineering

University of Wisconsin-Madison, 1415 Engineering Dr, Madison, WI 53706, USA

## Abstract

We analyze economic opportunities for industrial facilities provided by frequency regulation (FR) markets. We use classical frequency domain analysis techniques to characterize the harmonic content of FR signals and to analyze the impact of such harmonics on the response of dynamical systems. The analysis reveals that systems with slow dynamics, as thus found in large industrial systems, are suitable to provide FR capacity because they can naturally damp the dominant high-frequency harmonic content of FR signals. We also propose optimization formulations to quantify the maximum amount FR capacity that can be provided by a given system given its dynamic characteristics, its control structure, and FR dispatch signals. A distillation case study demonstrates that enormous economic potential exists for large industrial systems.

**Keywords:** electricity markets, frequency regulation, dynamics, manufacturing, control.

## 1 Introduction

Electricity markets are hierarchical decision-making processes that seek to coordinate generation, transmission, and consumption resources at multiple timescales. Figure 1 shows the major market layers, products, and timescales for the California Independent System Operator (CAISO). These markets exchange two general types of products: electrical energy and ancillary service capacity. Electrical energy is sold at three different timescales: in the Day-Ahead Market (DAM) with 1-hour intervals, in the Fifteen-Minute Market (FMM) with 15-min intervals, and in the Real Time Dispatch Process (RTPD) with 5-min intervals. The FMM and RTPD layers are also known as the Real-Time Market (RTM). The process of determining the resource dispatch schedule and locational (nodal) prices from bids is known as market clearing. Market clearing for the DAM occurs around noon of each preceding day. The RTM market corrects for errors in the original DAM schedule (which often arise from forecasting inaccuracies). As a result, RTM prices are more volatile and provide economic opportunities for market participants with dynamic (ramping) flexibility [16]. Electricity markets across the U.S. include both DAM and RTM processes but layer names, timescales, and specific rules may vary by region.

---

\*Corresponding Author: victor.zavala@wisc.edu

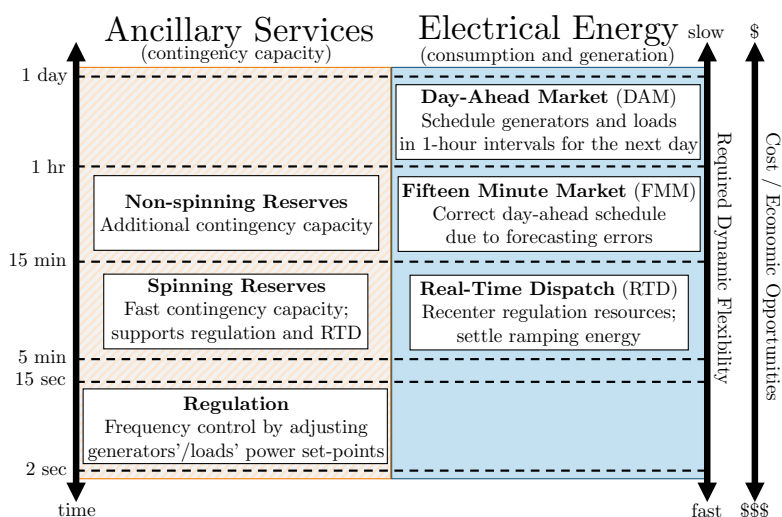


Figure 1: Market-based control hierarchy for the power grid. Resources may participate via multiple ancillary service and energy products [16].

30 In addition to energy products, resources can also provide flexibility in the form of *ancillary ser-*  
 31 *vices* such as frequency regulation, spinning reserves, and non-spinning reserves. In contrast to en-  
 32 ergy transactions (with prices in \$ / MWh), ancillary services are a contingency product, where re-  
 33 sources are paid for providing power capacity (with price in \$ / MW). Reserve capacities provide a  
 34 contingency in the event of unforeseen events that cannot be met by RTM (e.g., wind and solar supply  
 35 variations and generator failures). For example, a resource providing *spinning reserves* in CAISO is  
 36 contractually obligated to fully respond within 10 minutes of dispatch and provide 30 to 60 minutes  
 37 of power at the awarded reserve capacity. Requirements for *non-spinning reserves* are less stringent,  
 38 which allows resources with less dynamic flexibility to participate. Dispatch of reserves is rare; for  
 39 example, Alcoa reported 55 dispatches of reserves per year for a facility providing interruptible loads  
 40 (similar to reserve capacity) in the Midcontinent ISO [32,33].

41 The *frequency regulation* (FR) ancillary service helps balance the grid on the seconds to minutes  
 42 timescales. As the name suggests, FR is needed to keep the frequency of the grid at a required level  
 43 (60 Hz in the U.S.). Resources provide FR capacity offer a *flexibility band* to the market. Every 2 to 15  
 44 seconds, the Automatic Generator Control (AGC) system sends each resource providing FR capacity  
 45 a new power set-point (FR dispatch signal) within the flexibility band. Each resource is compensated  
 46 for both the size of the band (i.e., the capacity provided in MW) and also the amount of variability  
 47 in the FR dispatch signal. The variability is known as *mileage* and is defined as the absolute distance  
 48 between consecutive power set-points. Figure 2 shows the set-point and mileage for a hypothetic  
 49 generator providing FR capacity. The flexibility band is split into regulation up and regulation down  
 50 capacities, which are priced separately in some markets such as CAISO and the Electric Reliability  
 51 Council of Texas (ERCOT). The nominal set-point is the scheduled power output as set by an energy  
 52 market (e.g., DAM). Compared to reserves, providing FR capacity requires *significantly more dynamic*  
 53 *flexibility* from generators and loads. As a result, FR capacity is the most expensive ancillary service  
 54 (by a factor of two or more compared to reserves). For example, in the case of CAISO for the year of

55 2015, the average FR capacity price was \$ 5.72 / MW, compared to \$2.84 / MW and \$ 0.30 / MW for  
 56 spinning and non-spinning reserve capacity, respectively.

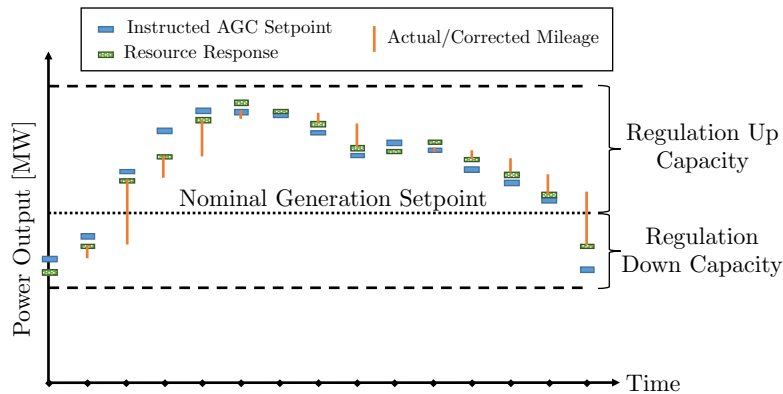


Figure 2: Illustration of FR dispatch signal, flexibility (capacity), and mileage [16].

57 Several industrial facilities already exploit economic opportunities from electricity markets. For  
 58 example, in ERCOT, load resources provide 2,400 MW of flexible capacity, including over half of the  
 59 spinning reserves. Notably, over 1,000 MW of this capacity is provided by a single electrochemical  
 60 manufacturing facility. Of the remaining capacity, 820 MW and 520 MW are provided by medium  
 61 (10 to 50 MW) to small (less than 10 MW) industrial and commercial loads, respectively. In the year  
 62 of 2015, a load could have saved 400,000 \$ / yr in CAISO by shifting 10 MW of consumption from  
 63 during the 1% most extreme RTM prices (between 97 and 1621 \$ / MWh) to the average price (30  
 64 \$ / MWh). Similarly, a load providing 10 MW of FR capacity for every hour would have received  
 65 500,000 \$ / yr in capacity payments [16].

66 The demand and prices for ancillary services is increasing, driven by high frequency variations of  
 67 non-dispatchable renewable resources (e.g., solar, wind) [24,29,35]. In light of these economic oppor-  
 68 tunities, single sites often participate in multiple demand response (DR) programs and ISO markets.  
 69 For example, Alcoa’s aluminum smelter in Warrick, IN provides 70 MW of FR capacity to the Mid-  
 70 continent ISO market. This represents 15% of the average load (470 MW) for the system. The same  
 71 facility also provides 75 MW of interruptible load (a separate DR program) [32,33]. According to the  
 72 Energy Information Administration (EIA), U.S. industry consumed 846 TWh of electricity in 2010,  
 73 with 71.7% of the demand arising from six major sectors: chemicals (22.1%), primary metals (14.5%),  
 74 paper (12.2%), food (9.6%), petroleum and coal products (7.8%), and plastics and rubber products  
 75 (5.4%) [1]. A recent analysis of CAISO data reveals that substantial economic opportunities for in-  
 76 dustrial systems that can provide flexibility at fast timescales (RTM and FR) [16]. For example, for  
 77 battery and CHP systems, it has been found that 60% to 90% of potential revenues are only accessible  
 78 through RTM. Similarly, providing ancillary services can increase revenues 40% to 100% relative to  
 79 only transacting energy. Consequently, the ISOs can greatly benefit from more active participation of  
 80 these sectors in electricity markets.

81 Applications for industrial demand response include combined heat and power (CHP) utility  
 82 plants [2,12,13,15,20,28,31], steel furnaces [3,11], cement plants [9,10,13,27,34], air separation units [7,  
 83 8,22,23,27,30,39,40,46,47,47], electrochemical manufacturing facilities [5], and pulp mills [18]. Early

84 literature focused on augmenting production scheduling frameworks to incorporate time-varying  
85 energy prices [4, 14]. Initial extensions considered uncertainty future electricity using stochastic pro-  
86 gramming formulations [18, 22]. More recent work also considered uncertain product demands [37]  
87 as well as robust optimization formulations [34, 39, 40]. Time is typically discretized into one hour or  
88 longer intervals that correspond with prices from DAM or time-of-day pricing schemes in one day or  
89 one week planning horizons [38]. All of these modeling approaches assume steady-state operation  
90 and thus neglect process dynamics. Although this is a reasonable assumption for participation in  
91 DAM, dynamics are essential for ancillary services operating at faster timescales. As such, multiscale  
92 modeling approaches are becoming increasingly relevant.

93 Different approaches have been proposed to incorporate process dynamics into production schedul-  
94 ing models, with cryogenic air separation units (ASUs) being one of the most relevant applica-  
95 tions [8, 30, 39, 40]. These systems produce purified oxygen, nitrogen, and argon by distillation  
96 with two or three mass and heat integrated columns. The separation is energy intensive due to the  
97 refrigeration needs, with compressor electrical loads reaching levels of up to 100 MW for large sys-  
98 tems. As such, important economic opportunities from RTM and FR markets are available for these  
99 systems. Unfortunately, it is a common perception in the chemical industry that systems exhibiting  
100 slow dynamics such as ASUs (time constants on the order of several hours) are not suitable for RTM  
101 and FR markets because they will not be able to track fast-varying dispatch signals. The majority of  
102 ancillary service capacity, however, is in fact provided by large equipment units such as aluminum  
103 smelters [41, 42] and electric arc furnaces [43]. The reason for these systems can *tolerate* fast variations  
104 in electrical energy input with negligible impact on product quality. In other words, in these systems  
105 *FR signals are treated as disturbances and not as tracking signals*.

106 An increasing share of ancillary service capacity is provided by energy storage technologies, such  
107 as batteries, that can provide power within less than a second [19]. Because the flexibility of these  
108 systems is well known, literature focuses on bidding strategies under uncertainty and simultaneous  
109 provision of multiple products. To this effect, we recently proposed an optimization framework for  
110 participation in multiple product markets (energy and ancillary services) at multiple timescales (day-  
111 ahead and real-time) [16]. Several recent studies explore providing ancillary services from building  
112 heat and cooling systems [6, 21, 44, 45]. In one study, Lin et al [25] demonstrate the feasibility of mod-  
113 ulating fan power consumption at fast frequencies ( $10^{-2}$  to  $10^{-3}$  Hz) to provide FR capacity while not  
114 disturbing chiller operation ( $10^{-4}$  Hz and slower). A recent study has also explored the possibility  
115 of coordinating millions of pool pumps in Florida to provide FR capacity at a large scale [26]. In this  
116 work we argue that similar ideas can be applied to traditional chemical processes such as distillation  
117 towers, pipelines, and cooling towers by noticing that load flexibility can be provided by mechanical  
118 equipment, pumps, fans, electric heaters, or steam supply (from CHP generation). The withstanding  
119 question is, however, *to what extent can chemical processes tolerate high-frequency electrical load fluctu-*  
120 *ations*. In order to address this question, we use classical frequency domain analysis techniques to  
121 characterize the harmonic content of FR signals and to analyze the impact of such harmonics on the  
122 response of dynamical systems. The analysis is used to illustrate that systems with slow dynam-  
123 ics, as thus found in large chemical processes, are suitable to provide FR capacity because they can  
124 naturally damp the dominant high-frequency harmonic content of FR signals. We also propose sim-

125 ple and rigorous strategies to quantify the maximum amount FR capacity that can be provided by a  
 126 given system given its dynamic characteristics, its control structure, and FR dispatch signals. A sim-  
 127 ple first-order system and a distillation case study demonstrate that enormous economic potential  
 128 exists for large industrial systems.

129 The paper is organized as follows. Section 2 reviews classical frequency domain analysis tech-  
 130 niques to analyze the response of a given dynamical system to harmonic signals. Section 3 analyzes  
 131 the frequency spectrum of FR signals and prices from historical data from ERCOT and CAISO mar-  
 132 kets. Section 4 presents an optimization formulation to determine the maximum FR capacity that a  
 133 given dynamical system can provide. Section 5 provides case studies to illustrate the concepts while  
 134 Section 6 outlines conclusions and future work.

## 135 2 Frequency Domain Analysis

We begin our discussion by analyzing the response of a dynamical system to harmonic signals. We use the following scalar system in the frequency domain:

$$y(j\omega) = H(j\omega)d(j\omega) \quad (2.1)$$

where  $\omega \in \mathbb{R}$  is the frequency,  $j := \sqrt{-1} \in \mathbb{C}$ ,  $d(j\omega) \in \mathbb{C}$  is the input disturbance,  $y(j\omega) \in \mathbb{C}$  is the output, and  $H : \mathbb{C} \rightarrow \mathbb{C}$  is the transfer function. We recall that the transfer function can be expressed as a phasor  $H(j\omega) = |H(j\omega)|e^{\angle H(j\omega)}$  or in rectangular form  $H(j\omega) = \Re H(j\omega) + j \cdot \Im H(j\omega)$ . It is well-known that the response of a stable system  $H(j\omega)$  (i.e., with stable poles) to a sinusoidal input settles at a sinusoidal steady-state known as the ultimate period response (UPR). To see this, we recall that the ultimate system response can be expressed in the time domain by using the convolution form:

$$\hat{y}(t) = \int_0^\infty h(\tau)d(t - \tau)d\tau \quad (2.2)$$

where  $h : \mathbb{R} \rightarrow \mathbb{R}$  is the inverse Laplace transform of  $H(\cdot)$ . If we define  $d(t) = A \cdot \sin(\omega t)$  (where  $A \in \mathbb{R}$  is the amplitude of the input signal) and recall from the Euler's identities that  $\sin(\omega t) = \frac{1}{2j}(e^{j\omega t} - e^{-j\omega t})$ , we can establish that:

$$\begin{aligned} \hat{y}(t) &= \int_0^\infty h(\tau)A \sin(\omega(t - \tau))d\tau \\ &= \frac{A}{2j} \int_0^\infty h(\tau)(e^{j\omega t} - e^{-j\omega t})d\tau \\ &= \frac{A}{2j} \int_0^\infty h(\tau)e^{j\omega t} - \frac{A}{2j} \int_0^\infty h(\tau)e^{-j\omega t}d\tau \\ &= \frac{A}{2j} e^{j\omega t} H(j\omega) - \frac{A}{2j} e^{-j\omega t} H(-j\omega) \\ &= \frac{A}{2j} e^{j\omega t} (\Re H(j\omega) + j\Im H(j\omega)) - \frac{A}{2j} e^{-j\omega t} (\Re H - j\Im H(j\omega)) \\ &= \frac{A}{2j} \Re H(e^{j\omega t} - e^{-j\omega t}) + \frac{A}{2} \Im H(e^{j\omega t} + e^{-j\omega t}) \\ &= A\Re H \sin(\omega t) + A\Im H \cos(\omega t) \\ &= A|H(j\omega)| \sin(\omega t + \angle H(j\omega)) \end{aligned}$$

In other words, the UPR is a sinusoidal response with amplitude  $A|H(j\omega)|$  and phase  $\angle H(j\omega)$ . Similarly, if we define the disturbance signal  $d(t) = A \cdot \cos(\omega t)$  and recall that  $\cos(\omega t) = \frac{1}{2}(e^{j\omega t} + e^{-j\omega t})$ , we can establish that:

$$\begin{aligned}
 \hat{y}(t) &= \int_0^\infty h(\tau) A \cos(\omega(t - \tau)) d\tau \\
 &= \frac{A}{2} \int_0^\infty h(\tau) (e^{j\omega t} + e^{-j\omega t}) d\tau \\
 &= \frac{A}{2} \int_0^\infty h(\tau) e^{j\omega t} + \frac{A}{2} \int_0^\infty h(\tau) e^{-j\omega t} d\tau \\
 &= \frac{A}{2} e^{j\omega t} H(j\omega) + \frac{A}{2} e^{-j\omega t} H(-j\omega) \\
 &= \frac{A}{2} e^{j\omega t} (\Re H(j\omega) + j\Im H(j\omega)) + \frac{A}{2} e^{-j\omega t} (\Re H - j\Im H(j\omega)) \\
 &= \frac{A}{2} \Re H (e^{j\omega t} + e^{-j\omega t}) + \frac{A}{2} j\Im H (e^{j\omega t} - e^{-j\omega t}) \\
 &= A \Re H \cos(\omega t) - A \Im H \sin(\omega t) \\
 &= A |H(j\omega)| \cos(\omega t + \angle H(j\omega))
 \end{aligned}$$

For any disturbance signal of the form

$$d(t) = \sum_{k=0}^N (A_k \sin(\omega_k t) + B_k \cos(\omega_k t)), \quad (2.3)$$

where  $A_k \in \mathbb{R}$  and  $B_k \in \mathbb{R}$  are the amplitude coefficients corresponding to frequency  $\omega_k \in \mathbb{R}$ , we have that the UPR is given by:

$$\hat{y}(t) = \sum_{k=0}^N |H(j\omega_k)| (A_k \sin(\omega_k t + \angle H(j\omega_k)) + B_k \cos(\omega_k t + \angle H(j\omega_k))). \quad (2.4)$$

136 Consequently, the UPR can be expressed as a sum of harmonics covering a given frequency spectrum.

For a first-order system of the form  $H(j\omega_k) = \frac{K}{\tau(j\omega_k + 1)}$ , with gain  $K \in \mathbb{R}$  and time constant  $\tau \in \mathbb{R}_+$ , we have that:

$$|H(j\omega_k)| = \frac{|K|}{\sqrt{(\omega_k \tau)^2 + 1}} \quad (2.5a)$$

$$\angle H(j\omega_k) = -\tan^{-1} \omega_k \tau. \quad (2.5b)$$

137 We can thus see that for a system with *fast dynamics* (i.e.,  $\tau \rightarrow 0$ ) we have that  $|H(j\omega_k)| \rightarrow |K|$  while  
 138 for a system with *slow dynamics* (i.e.,  $\tau \rightarrow \infty$ ) we have  $|H(j\omega_k)| \rightarrow 0$ . In other words, as the *system*  
 139 *becomes slower, it naturally damps the disturbance signal* (the amplitude of the UPR becomes smaller).  
 140 If we interpret the origin as a given reference steady-state, this indicates that a slower system will  
 141 exhibit small deviations from the reference point even in the face of a strong disturbance signal. We  
 142 also note that a system with a given time constant  $\tau$  is strongly affected by frequencies  $\omega_k$  smaller  
 143 than  $\mathcal{O}(\tau^{-1})$ . Consequently, if  $\tau$  is large (say  $\mathcal{O}(10)$ ) and the harmonic content of a disturbance signal  
 144 is dominated by frequencies larger than  $\mathcal{O}(\tau^{-1})$  (measured in terms of the magnitude coefficients  $A_k$

145 and  $B_k$ ), we can expect the dynamical system to be rather insensitive to the disturbance. These con-  
 146 cepts are illustrated in Figure 3, where we present the UPR of a first-order system with two different  
 147 time constants ( $\tau = 1$  and  $\tau = 10$ ) to a disturbance composed of two harmonics ( $\omega_1 = 1$  and  $\omega_2 = 10$ ).  
 148 Note that the slower system with  $\tau = 10$  damps the harmonics more strongly.

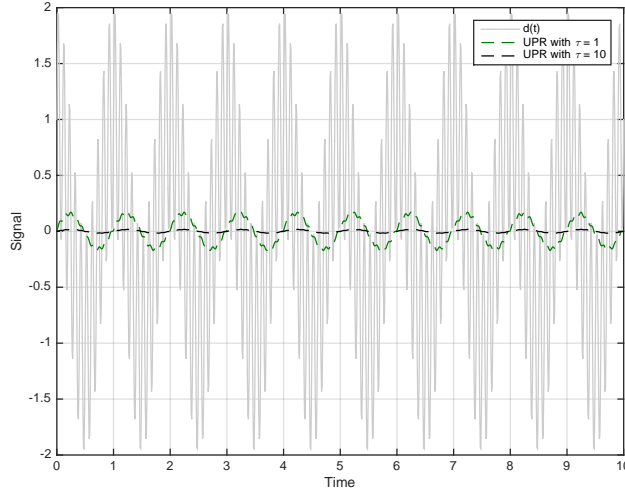


Figure 3: UPR for a fast and slow first-order system.

### 149 3 Analysis of Market Data

150 ISOs generate and disclose enormous amounts of market data. For example, CAISO generates over  
 151 1 trillion price data points each year, all of which are available through [oasis.caiso.com](http://oasis.caiso.com). This data  
 152 volume reflects the underlying complexity of market operations. In particular, energy prices are  
 153 set at three timescales (1-hour, 15-min, 5-min intervals) and vary spatially due to the transmission  
 154 network topology. The CAISO system contains over 8,000 nodes and each node has three locational  
 155 marginal prices for energy at every instance in time (one for each market layer). In contrast, ancillary  
 156 service prices are often set for a few regions (hubs) or are spatially uniform for the entire network.  
 157 In addition to prices, ISOs often release aggregate bid data, network information (nodes type, name,  
 158 GPS coordinates), and historical FR dispatch signals. As we show next, when combined with system  
 159 engineering techniques, these datasets can offer valuable insights for industrial market participants  
 160 on economic potential of market participation and for ISOs on incentives provided by market signals.

161 To identify the potential of an industrial dynamical system to participate electricity markets, we  
 162 begin by identifying the dominant timescales in the market signals. To do this, we represent market  
 163 price signals,  $\pi(t)$ , using Fourier expansions of the form:

$$\pi(t) = \sum_{k=0}^N A_k \sin(\omega_k t) + B_k \cos(\omega_k t), \quad (3.6)$$

164 The magnitude of the corresponding frequency domain signal at frequency  $\omega_k$  is given by:

$$|\pi(j\omega_k)| = \sqrt{A_k^2 + B_k^2}. \quad (3.7)$$

165 Figure 4 shows the frequency spectrum of historical IFM, FFM, and RTPD energy prices near Daggett,  
 166 CA in 2015. We have found that, in all three markets, 97% of the total signal magnitude (given by  
 167  $\sum_{k=0}^N |\pi(j\omega_k)|$ ) arises from frequencies larger than  $10^{-5}$  Hz (which correspond to day-to-day vari-  
 168 ations). Most notably, 60% of the total magnitude of IFM price signal (15-min price intervals) and  
 169 95% of the total magnitude of the RTPD price signal (5-min price interval) arises from frequencies  
 170 smaller than  $10^{-4}$ Hz (which corresponds to 2.75 hour periods). This illustrates that industrial sys-  
 171 tems seeking to participate in these energy markets must be capable of adjusting electrical loads at  
 172 similar timescales.

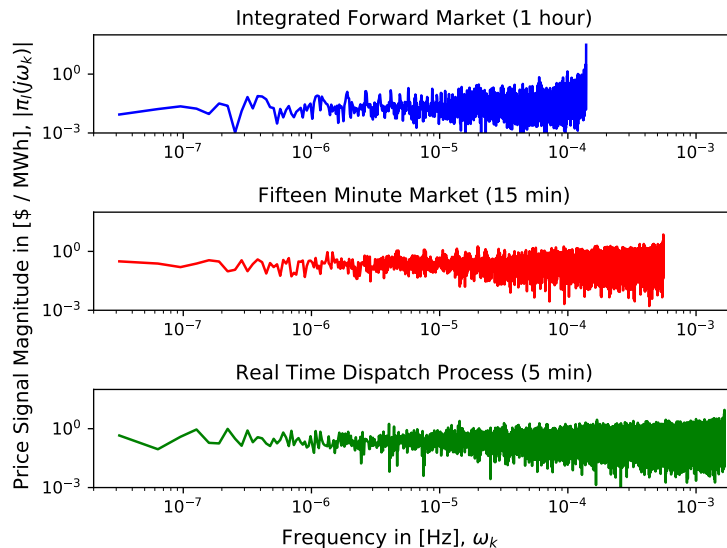


Figure 4: Frequency spectrum for CAISO energy prices near Daggett, CA in 2015.

173 Industrial systems seeking to provide FR capacity must also be concerned with dynamics of the  
 174 FR dispatch signal. ERCOT currently discloses historical FR dispatch signals for the first eleven days  
 175 of each month from July 2015 to June 2016<sup>1</sup>. These datasets include the system-wide dispatch sig-  
 176 nal and the total available FR capacity (both in MW) for regulation up and down products. We use  
 177  $\beta_+(t) \geq 0$  and  $\beta_-(t) \geq 0$  to represent the regulation up (RU) and regulation down (RD) dispatch sig-  
 178 nals, respectively, which are expressed as a fraction of the available capacity. Note that these signals  
 179 are mutually exclusive (i.e.,  $\beta_+(t) \cdot \beta_-(t) = 0$ ). Similar to the price signals, the harmonic content of the  
 180 total FR dispatch signal  $\beta(t) = \beta_+(t) - \beta_-(t)$  can be obtained by using a Fourier expansion. Figure 5  
 181 shows the FR signal for ERCOT in year 2016 both as a time series and decomposed into its harmonic  
 182 components. This ISO updates individual resource electrical power set-points every 4 seconds (0.25  
 183 Hz). We have found that approximately 70% of the total magnitude of the FR dispatch signal arises from

<sup>1</sup><http://www.ercot.com/mktrules/pilots/frfs>



184 frequencies between  $10^{-2}$  Hz (1.7 min period) and  $10^{-4}$  Hz (16.7 min period). This indicates that, in prin-  
 185 ciple, chemical processes can absorb most of the harmonic content of FR dispatch signals because equipment  
 186 usually have time constants on the order of minutes to hours. Moreover, as we will see in the next  
 187 sections, industrial systems are usually equipped with robust control architectures that are designed  
 188 to suppress a wide variety of disturbances.

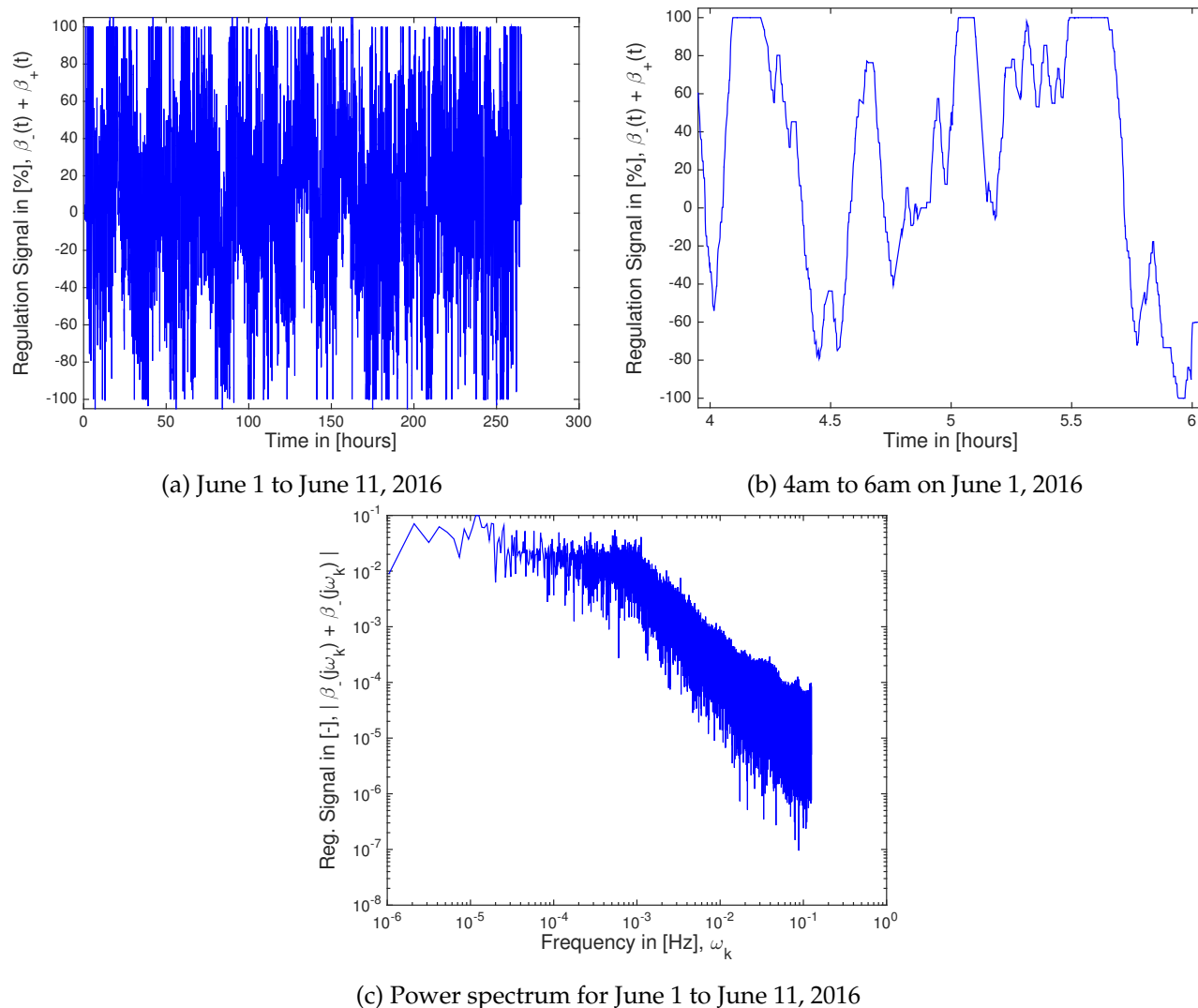


Figure 5: System-wide FR dispatch signals and spectrum for ERCOT for June 1st-11th, 2016.

189 A key question is whether mileage payments are important in FR markets. Recall that resources  
 190 providing FR are compensated for both capacity (size of the flexibility band) and mileage. The lat-  
 191 ter accounts for the variability of the FR dispatch signal. Table 1 shows regulation capacities prices,  
 192 mileage amounts, mileage prices, and mileage revenues for the CAISO DAM market (1-hour inter-  
 193 vals). CAISO only releases the average mileage for each hour per unit of FR capacity. Using these  
 194 data, we compute the anticipated revenue from mileage. Table 1 reports quantiles to summarize the  
 195 distributions of each quantity over the year. We see that, between the 0.0 to 0.6 quantiles, mileage

196 revenue is less than 3% of the overall capacity revenue. At the highest prices and mileage dispatch  
 197 (1.0 quantile), mileage revenues become significant. These results indicate that neglecting mileage  
 198 payments will not incur a large penalty. It is important to highlight, however, that this conclusion is  
 199 based on the average mileage allocation.

Table 1: Summary of FR capacity and mileage prices in CAISO during 2015. RD and RU stand for regulation down and up, respectively. Data obtained from [oasis.caiso.com](http://oasis.caiso.com).

	Quantile					
	0.0	0.2	0.4	0.6	0.8	1.0
RD Capacity Price (\$ / MW cap.)	0.0	1.74	2.62	3.27	3.91	58.88
RD Miles Amount (MW miles / MW cap.)	0.0	2.07	3.9	5.74	8.53	32.68
RD Miles Price (\$ / MW miles)	0.0	0.01	0.01	0.01	0.1	6.83
RD Miles Revenue (\$ / MW cap.)	0.0	0.02	0.06	0.11	0.44	12.56
RU Capacity Price (\$ / MW cap.)	0.0	1.55	2.23	3.99	7.84	55.24
RU Miles Amount (MW miles / MW cap.)	0.0	0.25	0.97	2.53	4.75	30.99
RU Miles Price (\$ / MW miles)	0.0	0.0	0.0	0.01	0.01	37.26
RU Miles Revenue (\$ / MW cap.)	0.0	0.0	0.0	0.02	0.06	92.62

## 200 4 Optimal Frequency Regulation Provision

Our goal is to quantify the maximum amount of FR capacity that a system can provide in order to maximize FR revenue while maintaining operational constraints (safety bounds, set-point deviations, product quality, wear-and-tear, and so on). We do this by posing an optimization problem of the form:

$$\min_{r_+(\cdot), r_-(\cdot), u(\cdot)} \int_{\mathcal{T}} \phi(z(t), u(t), d(t)) dt \quad (4.8a)$$

$$\text{s.t. } \dot{z}(t) = f(z(t), u(t), d(t)), \quad t \in \mathcal{T} \quad (4.8b)$$

$$y(t) = h(z(t)), \quad t \in \mathcal{T} \quad (4.8c)$$

$$g(z(t), y(t), u(t)) \leq 0, \quad t \in \mathcal{T} \quad (4.8d)$$

$$d(t) = r_+(t)\beta_+(t) - r_-(t)\beta_-(t), \quad t \in \mathcal{T} \quad (4.8e)$$

$$0 \leq r_+(t), r_-(t) \leq \alpha, \quad t \in \mathcal{T}. \quad (4.8f)$$

201 where  $\mathcal{T}$  is the time domain,  $z(t) \in \mathbb{R}^{n_z}$  are the states at time  $t$ ,  $y(t) \in \mathbb{R}^{n_y}$  represents the outputs,  
 202  $u(t)$  are the controls, and  $d(t)$  are the disturbances. We highlight that this formulation is general and  
 203 considers multivariable dynamical systems and, for simplicity, we assume that the only disturbance  
 204 is the FR dispatch signal. The constraints (4.8d) capture operational limits; for instance, an operator  
 205 might be interested in imposing constraints on the maximum deviation of a system output  $y(t)$  from

206 a given desired steady-state  $\bar{y}$  of the form:

$$\|y(t) - \bar{y}\| \leq \epsilon, \quad t \in \mathcal{T}, \quad (4.9)$$

207 where  $\epsilon \in \mathbb{R}_+$  is a *flexibility margin* that measures the maximum allowable deviation (where  $\|\cdot\|$  is  
 208 any suitable norm). The FR dispatch signal  $d(t)$  is decomposed into its FR up component  $\beta_+(t) \in \mathbb{R}_+$   
 209 and its FR down component  $\beta_-(t) \in \mathbb{R}_+$ . Although the harmonic content of the FR signal is fixed,  
 210 the operator can manipulate its magnitude by adjusting the amount of FR up and down capacity  
 211 provided to the market, which is represented by the variables  $r_+(t) \in \mathbb{R}_+$  and  $r_-(t) \in \mathbb{R}_+$ . These  
 212 capacities are bounded by the parameter  $\alpha \in \mathbb{R}_+$ . The objective function  $\phi(\cdot)$  captures revenue  
 213 from the FR market and other operational costs. The revenue collected from FR capacity is simply  
 214  $\int_{\mathcal{T}} (\pi_+(t)r_+(t) + \pi_-(t)r_-(t))dt$  where  $\pi_+(\cdot), \pi_-(\cdot)$  are the prices for regulation up and down capacity,  
 215 respectively. The prices  $\pi_+(t), \pi_-(t)$  and capacities  $r_+(t), r_-(t)$  are piece-wise (zero-hold) trajectories  
 216 where the length of the zero-hold period is one hour. The FR revenue can also potentially capture  
 217 mileage payments but we do not explore this aspect in this work because FR capacity is the most  
 218 dominant revenue item.

219 In summary, the goal of the proposed optimization formulation is to determine optimal trajec-  
 220 tories  $r_+(t), r_-(t), u(t), t \in \mathcal{T}$  that maximize the system economic objective function while satisfying  
 221 the constraints. Note that  $d(\cdot)$  acts as a disturbance and the system is remunerated for its ability to  
 222 counteract such disturbance by using the controls  $u(\cdot)$ . Consequently, the more flexibility the control  
 223 system has to counteract disturbances, the more FR revenue that can potentially be collected.

## 224 5 Case Studies

### 225 5.1 First-Order System

226 We first illustrate some of the concepts discussed by using an open-loop first-order system. This  
 227 seeks to highlight the interplay between the system dynamics, process flexibility, and FR revenue.  
 228 This analysis also gives a quick approach to estimate the FR revenue for a given first-order system.  
 229 A more sophisticated procedure for general dynamical systems is presented in Section 5.2.

230 Consider an input signal of the form  $d(t) = r \cdot \sin(\omega t)$ , where  $\omega$  and  $A$  are known parameters  
 231 that denote the frequency and amplitude of the FR signal. The ISO pays the industrial facility for  
 232 the FR capacity  $r \in \mathbb{R}_+$  at price  $\pi \in \mathbb{R}_+$  (same price for FR up and down capacity). We thus seek to  
 233 find  $r$  that maximizes the revenue  $\phi(r) = \pi \cdot r$  while keeping the magnitude of the UPR bounded as  
 234  $r \cdot A \cdot |H(j\omega)| \leq \epsilon$ . Here,  $\epsilon$  is a *flexibility margin* that captures the maximum allowable deviation from  
 235 a given steady-state. Since the UPR is symmetric and periodic, the UPR bound can also be written in  
 236 the time domain as  $\max_{t \in \mathcal{U}} |\hat{y}(t) - \bar{y}| \leq \epsilon$ , where  $\hat{y}(t)$  is the UPR and  $\mathcal{U}$  is the period of oscillation of  
 237 the UPR.

The FR revenue maximization problem can thus be written as:

$$\max_r \quad \pi \cdot r \quad (5.10)$$

$$\text{s.t.} \quad \frac{r \cdot A \cdot |K|}{\sqrt{(\omega\tau)^2 + 1}} \leq \epsilon. \quad (5.11)$$

Since  $r$  enters linearly in the objective and the constraint, the constraint is always active and we have that the optimal FR capacity provision is:

$$r^* = \frac{\epsilon \cdot \sqrt{(\omega\tau)^2 + 1}}{A |K|}. \quad (5.12)$$

Consequently, the optimal revenue is:

$$\phi(r^*) = \frac{\pi \cdot \epsilon \cdot \sqrt{(\omega\tau)^2 + 1}}{A |K|}. \quad (5.13)$$

238 As expected, the optimal revenue increases with increasing  $\tau$ , decreases with increasing  $|K|$ , and  
 239 increases with increasing flexibility margin  $\epsilon$ . We express the optimal revenue as an implicit function  
 240 of the flexibility  $r^*(\epsilon)$  and we let  $\alpha$  represent the maximum possible (ideal) FR capacity that can be  
 241 collected by the system. The bound  $\alpha$  is dictated by the system physical limits, such as the maximum  
 242 electric load that it can use. Applying this bound to (5.12) gives the optimal FR capacity:

$$r^*(\epsilon) = \min \left( \frac{\epsilon \cdot \sqrt{(\omega\tau)^2 + 1}}{A |K|}, \alpha \right). \quad (5.14)$$

243 Note that, without this bound, (5.12) has the property that, as  $A \rightarrow 0$ , the system can provide un-  
 244 bounded FR capacity (i.e.,  $r^*(\epsilon) \rightarrow \infty$ ). This gives unrealistic revenues for hours with small (or no)  
 245 FR dispatch. In contrast, (5.14) predicts  $r^*(\epsilon) \rightarrow \alpha$  as  $A \rightarrow 0$ . It is convenient to express the FR  
 246 capacity scaled by  $\alpha$ :

$$\hat{r}^*(\epsilon) = \frac{r^*(\epsilon)}{\alpha}, \quad (5.15)$$

247 which indicates the fraction of available FR capacity that can be utilized. When  $\hat{r}^*(\epsilon) < 1$ , system  
 248 dynamics limit participation in FR markets.

249 The optimal FR capacity can also be expressed as:

$$\hat{r}^*(\epsilon) = \min \left( \frac{\epsilon}{A \cdot \alpha \cdot \max_{t \in \mathcal{U}} |\hat{y}(t) - \bar{y}|}, 1 \right). \quad (5.16)$$

250 This representation is useful to evaluate FR revenues in the presence of more general FR dispatch sig-  
 251 nals that are composed of many frequencies. In particular, one can show that the maximum deviation  
 252 of the UPR from steady-state is bounded as:

$$\max_{t \in \mathcal{U}} |\hat{y}(t) - \bar{y}| \leq |K| \sum_{k=0}^N \frac{\sqrt{A_k^2 + B_k^2}}{\sqrt{(\omega_k\tau)^2 + 1}}. \quad (5.17)$$

253 By combining (5.16) and (5.17), we can obtain an estimate of the optimal FR provision as:

$$\hat{r}^*(\epsilon) \approx \min \left( \frac{\hat{\epsilon}}{\sum_{k=0}^N \frac{\sqrt{A_k^2 + B_k^2}}{\sqrt{(\omega_k\tau)^2 + 1}}}, 1 \right), \quad (5.18)$$

254 where we define the dimensionless flexibility margin:

$$\hat{\epsilon} = \frac{\epsilon}{A \cdot |K| \cdot \alpha}. \quad (5.19)$$

255 We note that this optimal FR provision estimate (5.18) can be computed explicitly (without any dy-  
 256 namic simulations) by using the spectrum information of the FR signal and the parameters of the  
 257 first-order system. One can compute an exact estimate of the optimal FR provision by explicitly  
 258 computing the bound  $\max_{t \in \mathcal{U}} |\hat{y}(t) - \bar{y}|$  through simulation of the UPR  $\hat{y}(t)$  over  $\mathcal{U}$ . This approach,  
 259 however, is computationally more expensive.

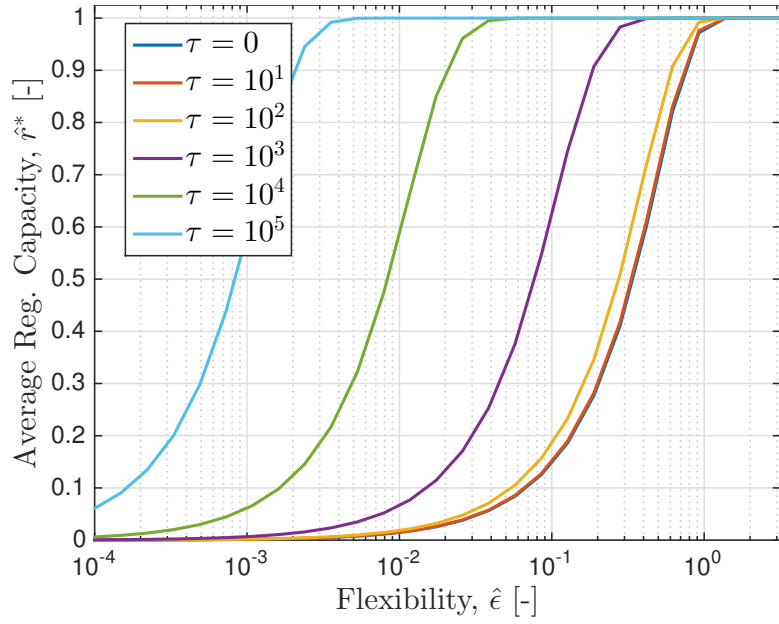
260 We use the FR provision estimate (5.18) to derive quick estimates of FR revenue for different first-  
 261 order systems using historical market data from ERCOT. The dynamical system is fully characterized  
 262 by the time constant  $\tau$  and the dimensionless flexibility  $\hat{\epsilon}$ . We apply a Fourier expansion of the FR  
 263 signal to obtain  $A_k, B_k$  and  $\omega_k$ . For each hour in the data set, the FR revenue is computed from the  
 264 provision estimate (5.18) and the prices  $\pi_+(t), \pi_-(t)$  from ERCOT. For hours with  $\beta_+(t) - \beta_-(t) = 0$ ,  
 265 we define  $\hat{r}^* = 1$ . The results are presented in Figure 6. For a given time constant  $\tau$ , the average  
 266 hourly FR capacity provision approaches one as the flexibility  $\hat{\epsilon}$  increases, as expected. The diminish-  
 267 ing returns are explained by the variation in FR dispatch from hour-to-hour. As the flexibility budget  
 268  $\hat{\epsilon}$  increases,  $\hat{r}^*(\hat{\epsilon})$  reaches the saturation point. For a given flexibility budget  $\hat{\epsilon}$ , slower systems (those  
 269 with larger  $\tau$ ) can provide greater FR capacity. This is because the amplitude of the UPR approaches  
 270 zero as  $\tau \rightarrow \infty$ . From Figure 6 we can also see that annual revenues predicted can reach up to \$140,000  
 271 for a system providing a single MW of FR capacity.

## 272 5.2 Water-Methanol Distillation System

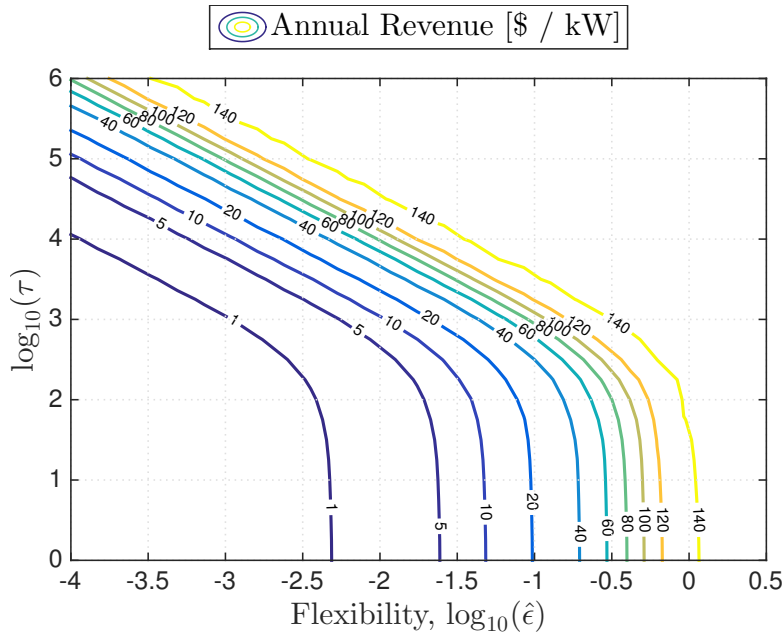
273 Previous studies reported in the literature have focused on providing FR services using energy sys-  
 274 tems with fast dynamics and large flexibility margins such as batteries, arc furnaces, aluminum  
 275 smelters, buildings, pumps, and so on. We argue that many other energy-intensive unit opera-  
 276 tions having slow dynamics can also be used for providing FR capacity. To see this, we consider  
 277 the distillation column system for an experimental binary water-methanol separation from Wood  
 278 and Berry [36]:

$$\begin{bmatrix} x_D(j\omega) \\ x_B(j\omega) \end{bmatrix} = \begin{bmatrix} \frac{12.8e^{-j\omega}}{16.7(j\omega)+1} & \frac{-18.9e^{-3j\omega}}{21.0(j\omega)+1} \\ \frac{-6.6e^{-7j\omega}}{10.9(j\omega)+1} & \frac{-19.4e^{-3j\omega}}{14.4(j\omega)+1} \end{bmatrix} \begin{bmatrix} R(j\omega) \\ S(j\omega) \end{bmatrix} \quad (5.20)$$

279 The outputs  $x_D(\cdot)$  and  $x_B(\cdot)$  are the distillate and bottoms compositions (in wt% methanol), respec-  
 280 tively. The input variables  $R(\cdot)$  and  $S(\cdot)$  are the reflux and steam flow rates (in lb/min), respectively.  
 281 The time constants are expressed in minutes and we thus highlight that the system has a relatively  
 282 slow response. The transfer functions (5.20) are built around deviations using the steady-state refer-  
 283 ence point  $x_D = 96.0, x_B = 0.5, R = 1.95, S = 1.71$ . We assume that the distillation system provides  
 284 FR capacity by allowing variations in the energy input (steam) flow rate  $S$ . Consequently, the steam  
 285 flow rate is treated as a disturbance. This can be realized in practice by either using an electric re-  
 286 boiler or by providing FR from a utility plant that supplies the steam. In the latter case, adjusting the  
 287 electricity output of the utility plant to track the FR signal would also result in variations in steam  
 288 flow rate that need to be absorbed by the distillation system. Wood and Berry report that the steam



(a) FR Capacity



(b) Annual FR Revenue

Figure 6: FR capacity allocations and revenues for first-order systems in ERCOT.

289 supply for their column is at 233.0 °F. Assuming that only the latent heat of vaporization is used, a 1.0  
 290 lb/min change in  $S$  is equivalent to a change of 956.6 Btu/min or 16.82 kW in the input energy flow  
 291 rate. This is important, as hourly regulation prices are reported in \$ / MW. We set the FR capacity to  
 292  $\alpha = 11.5$  kW, which corresponds to a 40% deviation from the steady-state steam flow rate.

293 **5.2.1 UPR Analysis Approach**

294 In order to apply the previous analysis for linear systems, we neglect the time delay, and focus solely  
 295 on the transfer functions relating  $S$  to  $x_D$  and  $x_B$ , and convert the units:

$$x_D(j\omega) = \frac{K_D}{\tau_D(j\omega) + 1}, \quad x_B(j\omega) = \frac{K_B}{\tau_B(j\omega) + 1} \quad (5.21)$$

296 where  $K_D = -1.12$  wt% per kW,  $\tau_D = 1.26 \times 10^3$  sec,  $K_B = -1.15$  wt% per kW,  $\tau_B = 8.64 \times 10^2$   
 297 sec. We also highlight that the column is bench-scale with a nominal reboiler duty of 28.8 kW. Figure  
 298 6 provides an estimate of potential FR market revenues obtained by using (5.18) on each individual  
 299 transfer function separately (neglecting variable interactions). We begin by considering a flexibility  
 300 margin of  $\epsilon = 1.0$  wt%, which corresponds to  $\hat{\epsilon} \approx 10^{-1}$ . Figure 6 predicts revenues near 80 \$/kW.  
 301 Table 2 shows results resulting from re-evaluating (5.18) with precise values for  $\hat{\epsilon}$  corresponding to  
 302 the distillation system. Figure 7 shows the results along with three cases (labelled as A, B, and C)  
 303 from Table 2. For  $x_D$ , we see that an order of magnitude change in the flexibility  $\epsilon$  (from 0.1 to 1.0  
 304 wt%) results in an order of magnitude change in revenues (8.6 to 83.3 \$/kW).

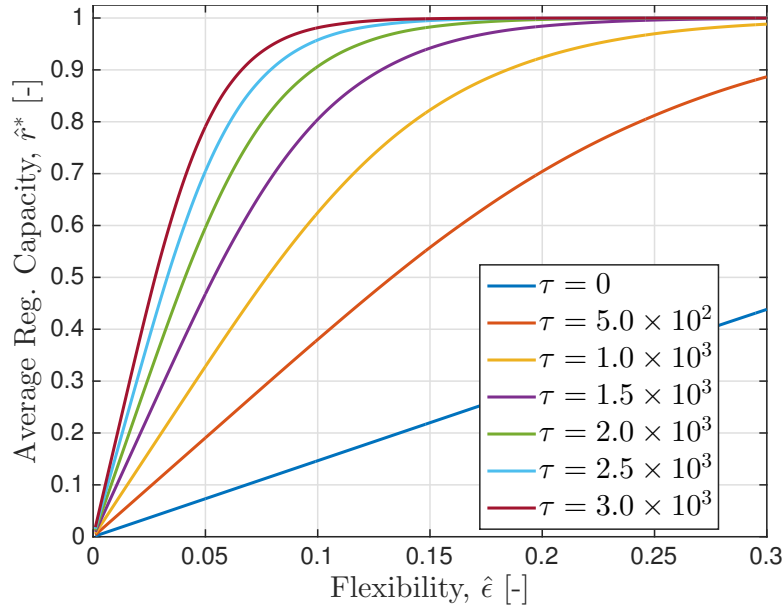
305 Figure 2 also offers interesting insights that can be used to guide the design of the distillation  
 306 system. Consider the goal of capturing revenues of 127.5 \$/ kW (which is 90% of available market  
 307 revenues). With a flexibility of  $\epsilon = 1.0$  wt% and  $K_D$  fixed, the time constant  $\tau_D$  would need to  
 308 be doubled. This can potentially be achieved by increasing material hold-ups. Alternatively, with  
 309  $\tau_D$  fixed,  $K_D$  would need to be halved or  $\epsilon$  would need to be doubled to 2.0 wt% to meet the 90%  
 310 revenue goal.

Table 2: Revenue estimates for distillation system from UPR analysis with historical ERCOT data.

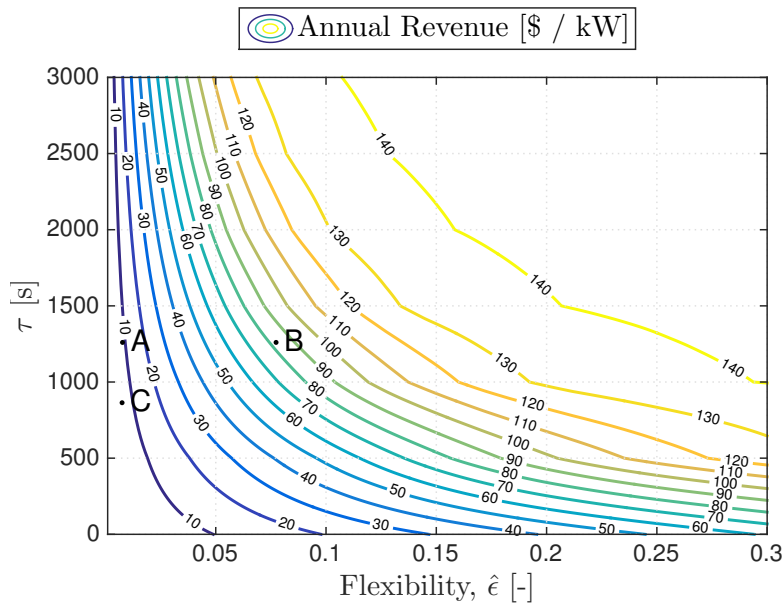
Case	Variable	$\epsilon$	$\hat{\epsilon}$	Avg. FR Capacity	Annual Revenue
A	$x_D$	0.1 wt%	$7.7 \times 10^{-3}$	6.2%	8.62 \$/kW
B	$x_D$	1.0 wt%	$7.7 \times 10^{-2}$	59.8%	83.34 \$/kW
C	$x_B$	0.1 wt%	$7.5 \times 10^{-3}$	4.2%	6.03 \$/kW

311 **5.2.2 Optimization Approach**

312 The UPR method provides rough estimates of potential FR revenue but is limited in that: (a) it con-  
 313 sider flexibility budgets  $\hat{\epsilon}$  in only one variable at a time (assuming decoupled dynamics), (b) it con-  
 314 sider only open-loop responses (i.e., the reflux flow rate  $R$  is not used to counteract disturbances in  
 315 the steam flow rate  $S$ ), (c) the analysis uses the UPR trajectory to compute the regulation capacity but  
 316 the system may not have enough time to settle, and (d) the formulation requires a prior specification  
 317 of the ratio of FR up and down capacity provisions. To overcome these limitations, we use the more  
 318 general optimization formulation (4.8). We consider a horizon of one hour (which matches pricing  
 319 and bidding mechanisms for most day-ahead markets). The dynamics (4.8b) are discretized with



(a) Regulation Capacity



(b) Annual Revenues

Figure 7: Optimal FR capacity provisions and revenues for distillation system (5.21) using UPR approach. Labels A, B, and C correspond to the cases in Table 2.

320 four second timesteps to match the FR dispatch signal update rates. For the implementation of (5.20)  
 321 in the time domain, we use a state-space representation of the form:



$$\begin{aligned}
 \mathbf{z}(t) &= \mathbf{A} \mathbf{z}(t-1) + \mathbf{B} \begin{bmatrix} R(t) \\ S(t) \end{bmatrix}, \\
 \mathbf{y}(t) &= \begin{bmatrix} x_D(t) \\ x_B(t) \end{bmatrix} = \mathbf{C} \mathbf{z}(t), \\
 \mathbf{A} &= \begin{bmatrix} 0.99602 & 0 & 0 & 0 \\ 0 & 0.9939 & 0 & 0 \\ 0 & 0 & 0.99683 & 0 \\ 0 & 0 & 0 & 0.99538 \end{bmatrix}, \\
 \mathbf{B} &= \begin{bmatrix} 0.066534 & 0 \\ 0.066463 & 0 \\ 0 & 0.066561 \\ 0 & 0.066513 \end{bmatrix}, \\
 \mathbf{C} &= \begin{bmatrix} 0.76647 & 0 & -0.9 & 0 \\ 0 & 0.6055 & 0 & -1.3472 \end{bmatrix}.
 \end{aligned} \tag{5.22}$$

The optimal FR capacity provision for a given hour is obtained by solving the discrete-time optimization problem:

$$\max_{\bar{S}, r_-, r_+, R} \quad r_+ \cdot \pi_+ + r_- \cdot \pi_- + \rho \sum_{t \in \mathcal{T}} |R(t) - R(t-1)| \tag{5.23a}$$

$$\text{s.t.} \quad \mathbf{z}(t) = \mathbf{A} \mathbf{z}(t-1) + \mathbf{B} \begin{bmatrix} R(t) \\ S(t) \end{bmatrix}, \quad t \in \mathcal{T}, \tag{5.23b}$$

$$\mathbf{y}(t) = \mathbf{C} \mathbf{z}(t), \quad t \in \mathcal{T}, \tag{5.23c}$$

$$S(t) = r_+ \beta_+(t) - r_- \beta_-(t) + \bar{S}, \quad t \in \mathcal{T}, \tag{5.23d}$$

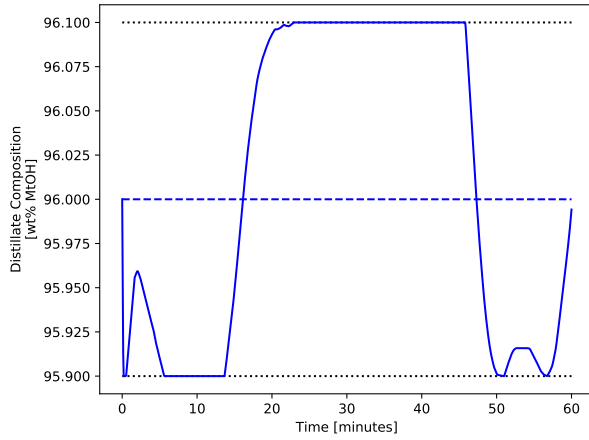
$$\underline{\epsilon} \leq \mathbf{y}(t) \leq \bar{\epsilon}, \quad t \in \mathcal{T}, \tag{5.23e}$$

$$|R(t)| \leq \delta, \quad t \in \mathcal{T}, \tag{5.23f}$$

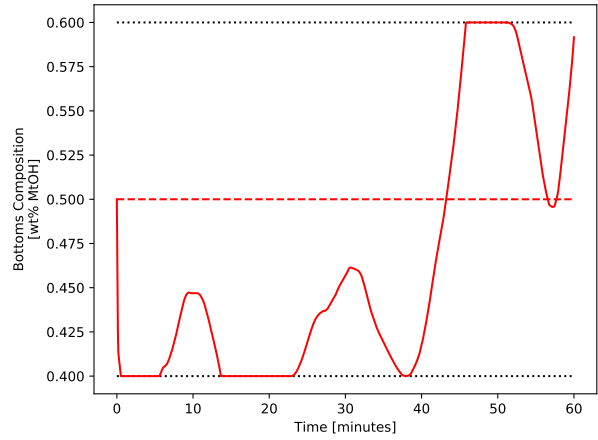
$$0 \leq r_+, r_- \leq \alpha. \tag{5.23g}$$

322 The decision variables include the FR down capacity  $r_-$ , FR up capacity  $r_+$ , the steam flow rate  
 323 offset  $\bar{S}$ , and the reflux flow rate  $R(t)$  for  $t \in \mathcal{T}$ . The objective includes a term to penalize changes  
 324 in the reflux flow rate to encourage gradual control actions and prevent wear-and-tear effects. Input  
 325 parameters include the FR down and up prices ( $\pi_-$  and  $\pi_+$ ), objective penalty ( $\rho = 10^{-5}$ ), and FR up  
 326 and down dispatch signals at each time step ( $\beta_-(t)$  and  $\beta_+(t)$ ). To improve scaling, the variables  $S$ ,  
 327  $r_-$ ,  $r_+$ , and  $\alpha$  are expressed in lb/min in (5.23). A one-hour horizon includes  $T=900$  time steps (one  
 328 hour discretized using four second timesteps) and we thus define the time set  $\mathcal{T} = \{1, \dots, T\}$  with  
 329  $R(0) = 0$  and  $\mathbf{z}(0) = \mathbf{0}$ . Problem (5.23) contains 7,202 variables with bounds, 5,401 linear equality  
 330 constraints, and 1,801 linear inequality constraints.

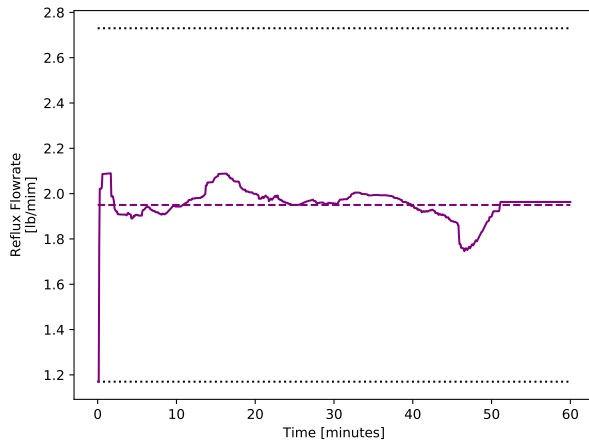
331 Figure 8 shows the optimal solution of (5.23) using market data from ERCOT, flexibility margins  
 332  $\underline{\epsilon} = (-0.1, -0.1)$  and  $\bar{\epsilon} = (0.1, 0.1)$  (in wt%), a bound on the reflux flow rate of  $\delta = 0.78$  lb/min (which



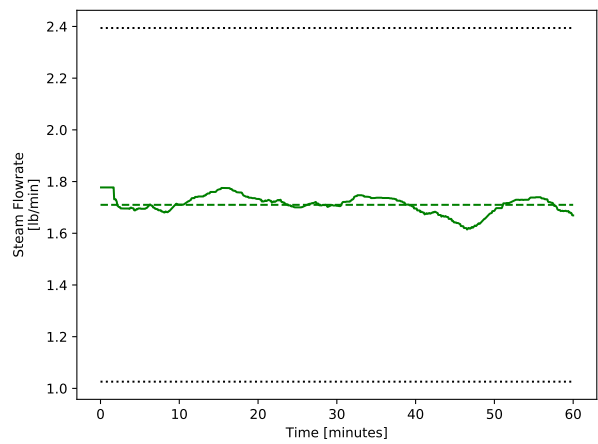
(a) Distillate Composition,  $x_D(t)$



(b) Bottoms Composition,  $x_B(t)$



(c) Reflux Flow rate,  $R(t)$



(d) Steam Flow rate,  $S(t)$

Figure 8: Results for (5.23) using ERCOT data for midnight to 1am, July 1st, 2015.

333 corresponds to 40% of the steady-state value) and a FR capacity bound  $\alpha = 11.5$  (in kW). The dashed  
 334 color lines indicate the steady-state values for each variable and the dotted black lines show bounds.  
 335 For this hour, the optimal market provisions are  $r_+^* = 1.2$  and  $r_-^* = 3.4$  (in kW). This asymmetric FR  
 336 capacity provisions stem from the higher price for FR down during this particular hour ( $\pi_- = 3.98$   
 337 and  $\pi_+ = 3.0$  in \$ / MW). The plots show that  $x_D(t)$  and  $x_B(t)$  hit their bounds, often more than  
 338 once during the hour. This is because the optimizer is manipulating these profiles to maximize the  
 339 FR revenues. The bounds on the steam flow rate  $S(t)$  in Figure 8d are not active in this hour. We  
 340 also note that the system dynamics limit capacity provisions at this hour. Moreover, as the flexibility  
 341 margins  $\underline{\epsilon}$  and  $\bar{\epsilon}$  are relaxed, the trajectories for the reflux flow rate  $R(t)$  hit the bounds more often.

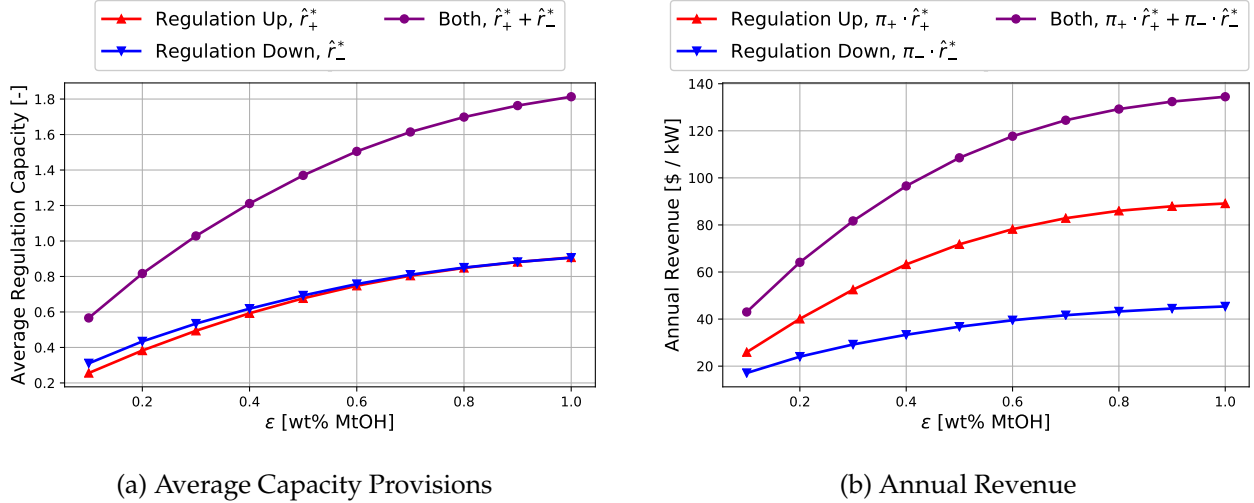


Figure 9: FR revenues as a function of flexibility for optimization approach.

342 To estimate revenues for an entire year we solve problem (5.23) for each hour. Here, flexibility  
 343 margins were set to  $\underline{\epsilon} = (-\epsilon, -0.1)$  and  $\bar{\epsilon} = (\epsilon, \epsilon)$  in wt%. Figure 9 shows the results for values of  $\epsilon$   
 344 from 0.1 to 1.0 wt%. The lower bound for the deviation of  $x_B$  is fixed at  $-0.1$  wt% to avoid negative  
 345 compositions (non-physical solutions). As expected, there are strong improvements in revenues for  
 346 additional flexibility. Notably, we notice that the maximum revenue predicted by the optimization  
 347 approach is on the order of 140,000 \$/MW, which is consistent with that obtained with the UPR  
 348 approach.

349 Figure 9a shows that, at  $\epsilon = 0.1$  wt%, average FR capacity provisions are 26% (for up capacity)  
 350 and 31% (for down capacity). By increasing the flexibility margin to  $\epsilon = 1.0$  wt% provisions increase  
 351 to 91% for both up and down capacities. For the same flexibility margins, total revenues span 43,000  
 352 \$/MW to 134,000 \$/MW (see Figure 9b). Interestingly, *average* FR provisions are almost identical  
 353 for up and down products (see Figure 9a). This is surprising given that the *average* price for FR up  
 354 capacity (10.60 \$ / MW) is twice the *average* price from down capacity (5.57 \$ / MW). Intuitively,  
 355 one would expect greater sales of the more valuable product. To further analyze this contradictory  
 356 result, problem (5.23) was resolved for each hour for  $\epsilon = 0.5$  wt% with  $r_-$  fixed to zero. With these  
 357 restrictions, the optimal provisions are 83.4% for up capacity, giving 77.1 \$/kW. In contrast, the op-

358 timization policy without the restriction sells 67.7% of up FR capacity for 71.8 \$/kW and 69.2% of  
359 down FR capacity for 36.8 \$/kW. Consequently, it is more lucrative to sell a blend of up and down  
360 FR capacities. This suggests that, although FR down capacity is twice as valuable as up capacity, it is  
361 also more difficult to provide. In other words, providing a unit of FR up capacity consumes a lesser  
362 amount of the total flexibility margin. Finally, it is important to note that the *average* FR capacities are  
363 nearly equal between up and down products, whereas the optimal ratio varies by hour depending  
364 on the price and FR dispatch signal. We also highlight that flexibility bands for the distillate and  
365 bottoms composition can potentially be expressed as average constraints, which can provide more  
366 flexibility.

367 Although the maximum possible FR revenues obtained with the the UPR and optimization ap-  
368 proaches are similar, the UPR analysis of Section 5.2.1 predicted capacity provisions between 4% and  
369 60% with revenues between 6,000 and 83,000 \$/MW, whereas the optimization approach (Section  
370 5.2.2) predicted capacity provisions between 26% and 91% with revenues between 43,000 to 134,000  
371 \$/MW. The difference is significant and stems from the assumptions used in the UPR technique. In  
372 particular, the UPR estimates neglect the ability to counteract the FR signal. In contrast, the optimiza-  
373 tion approach directly computes the best possible control strategy that mitigates the FR disturbance.  
374 To illustrate the effect of the additional flexibility gained with the control strategy, we solved (5.23)  
375 by setting  $\delta = 0$  (which fixes the control  $R(t) = 0$ ). The results, given in Table 3, indicate that the  
376 *control system can double to triple FR revenue*.

377 The  $\delta = 0$  optimization cases facilitate direct comparison with the results of Table 2. For  $\epsilon = 0.1$   
378 wt%, UPR analysis predicts revenues of 6,000 and 8,000 \$/MW, whereas the restricted optimization  
379 approach predicts 15,500 \$/MW. The difference in this case arises because the latter approach can *ad-*  
380 *just the blend of up and down FR capacity*. For  $\epsilon = 1.0$  wt%, the UPR analysis predicts revenue of 83,300  
381 \$/MW, whereas the optimization formulation yields 56,000 \$/MW. This difference is because the for-  
382 mer (Case B) only consider bounds on the  $x_D$  trajectory, whereas the latter considers bounds on both  
383  $x_D$  and  $x_B$  (including a tight lower bound on  $x_B$ ). Consequently, the UPR approach overestimates  
384 performance.

385 Because the optimization formulation is more general and flexible, it is preferred for detailed  
386 economic assessment. On the other hand, the UPR technique can be used to quickly assess the impact  
387 of the time constant  $\tau$  and flexibility  $\hat{\epsilon}$  on revenue. The UPR analysis also involves simple calculations.  
388 For instance, all of the computations for Figure 6 required less than 5 CPU-minutes in `Matlab`. In  
389 contrast, generating Figure 9 for the optimization approach required the solution of 31,690 instances  
390 of (5.23), which took 8.5 hours for CPU time. Problem (5.23) was implemented in `JuMP` [17] and  
391 solved with `Gurobi 7.0`.

392 To gain a perspective on the enormous *economic potential* for industrial-sized systems, we consider  
393 the following numbers. The annual methanol demand in 2015 was of around 70 million tonne per  
394 year, which was met by around 90 facilities world-wide<sup>2</sup>. This translates to an average methanol  
395 production of 33,000 lb/min per plant. Scaling-up the model of Wood and Berry [36] suggests a  
396 nominal *steam demand of 800 MW for distillation in an average methanol plant*. Using only 1% of this

---

<sup>2</sup><http://www.methanol.org/the-methanol-industry>

Table 3: Economic benefits of using reflux flow rate to counteract FR disturbance.

Flexibility	Adjust Reflux $R$ ?	FR Capacity		Annual Revenue
		Up	Down	
$\epsilon = 0.1$ wt%	No ( $\delta = 0$ lb/min)	9.0 %	13.9 %	15.5 \$/kW
	Yes ( $\delta = 0.78$ lb/min)	25.6 %	31.0 %	43.0 \$/kW
$\epsilon = 1.0$ wt%	No ( $\delta = 0$ lb/min)	31.2 %	40.8 %	56.1 \$/kW
	Yes ( $\delta = 0.78$ lb/min)	90.7 %	90.6 %	134.5 \$/kW

energy input for FR in each direction ( $\alpha = 8$  MW) could conservatively result in revenues of 320,000 \$ / year (computed from 40 \$/kW / year  $\times$  8,000 kW). Moreover, scaling up the production rate by a factor of  $10^4$  should slow down system dynamics (increase  $\tau$ ) and reduce the gain  $K$  (whose units are wt% per input energy). Both of these factors will increase the amount of FR capacity that can be sold. Thus the 40 \$/kW / year estimated for the laboratory-scale column with  $\epsilon = 0.1$  wt% is likely achievable with industrial size systems with a much tighter flexibility budget, as predicted by (5.19) and Figure 6. The maximum possible revenues for 8 MW of FR up and down capacity provided by the distillation system is in the order of 1.1 million \$ / year (based on ECROT data for 2015 and 2016).

## 6 Conclusions and Future Work

In this work, we have analyzed economic opportunities provided by frequency regulation (FR) markets to industrial systems. We use frequency domain analysis to highlight the dominant frequencies in FR dispatch signals and to argue that slow dynamical systems can naturally damp such frequencies. We propose a fast method to assess the FR revenue potential for open-loop dynamical systems and a more sophisticated optimization method to determine the maximum amount of FR provision that can be offered by a given industrial system while satisfying operational constraints. As part of future work, we are interested in accounting for uncertainty in prices and FR dispatch signals by using stochastic programming formulations and to assess the performance of different types of industrial-sized systems such as air separation units and cooling towers.

## Acknowledgments

We thank the Vice Chancellor for Research and Graduate Education at the University of Wisconsin-Madison and the industrial members of the TWCCC consortium for the generous support.

## References

- [1] Table 11.1 Electricity: Components of Net Demand, 2010. Technical report, U.S. Energy Information Administration, 3 2013.

- 421 [2] F. Al-Mansour and M. Kožuh. Risk analysis for CHP decision making within the conditions of  
422 an open electricity market. *Energy*, 32(10):1905–1916, 2007.
- 423 [3] S. Ashok. Peak-load management in steel plants. *Applied Energy*, 83(5):413–424, 2006.
- 424 [4] S. Ashok and R. Banerjee. An optimization mode for industrial load management. *IEEE Trans-*  
425 *actions on Power Systems*, 16(4):879–884, 2001.
- 426 [5] C. A. Babu and S. Ashok. Peak Load Management in Electrolytic Process Industries. *IEEE*  
427 *Transactions on Power Systems*, 23(2):399–405, 2008.
- 428 [6] F. Baccino, F. Conte, S. Massucco, F. Silvestro, and S. Grillo. Frequency Regulation by Manage-  
429 ment of Building Cooling Systems through Model Predictive Control. In *Power Systems Compu-*  
430 *tation Conference (PSCC)*, pages 1 – 7, 2014.
- 431 [7] Y. Cao, C. L. Swartz, M. Baldea, and S. Blouin. Optimization-based assessment of design lim-  
432 itations to air separation plant agility in demand response scenarios. *Journal of Process Control*,  
433 33:37 – 48, 2015.
- 434 [8] Y. Cao, C. L. E. Swartz, and J. Flores-Cerrillo. Optimal dynamic operation of a high-purity air  
435 separation plant under varying market conditions. *Industrial & Engineering Chemistry Research*,  
436 55(37):9956–9970, 2016.
- 437 [9] P. M. Castro, I. Harjunoski, and I. E. Grossmann. New Continuous-Time Scheduling Formu-  
438 lation for Continuous Plants under Variable Electricity Cost. *Industrial & Engineering Chemistry*  
439 *Research*, 48:6701–6714, 2009.
- 440 [10] P. M. Castro, I. Harjunoski, and I. E. Grossmann. Optimal scheduling of continuous plants with  
441 energy constraints. *Computers and Chemical Engineering*, 35(2):372–387, 2011.
- 442 [11] P. M. Castro, L. Sun, and I. Harjunoski. Resource-Task Network Formulations for Indus-  
443 trial Demand Side Management of a Steel Plant. *Industrial and Engineering Chemistry Research*,  
444 52(36):13046–13058, 2013.
- 445 [12] A. Christidis, C. Koch, L. Pottel, and G. Tsatsaronis. The contribution of heat storage to the prof-  
446 itable operation of combined heat and power plants in liberalized electricity markets. *Energy*,  
447 41(1):75–82, 2012.
- 448 [13] M. Coatalem, V. Mazauric, C. L. Pape-Gardeux, and N. Mazi. Optimizing industries’ power  
449 generation assets on the electricity markets. *Applied Energy*, 185, Part 2:1744 – 1756, 2017.
- 450 [14] B. Daryanian, R. Bohn, and R. Tabors. Optimal demand-side response to electricity spot prices  
451 for storage-type customers. *IEEE Transactions on Power Systems*, 4(3):897–903, 1989.
- 452 [15] M. De Paepe and D. Mertens. Combined heat and power in a liberalised energy market. *Energy*  
453 *Conversion and Management*, 48(9):2542–2555, 2007.

- 454 [16] A. W. Dowling, R. Kumar, and V. M. Zavala. A multi-scale optimization framework for electric-  
455 ity market participation. *Applied Energy*, 190:147–164, 2017.
- 456 [17] I. Dunning, J. Huchette, and M. Lubin. Jump: A modeling language for mathematical optimiza-  
457 tion. *SIAM Review*, 59(2):295–320, 2017.
- 458 [18] G. Everett and A. Philpott. Pulp electricity demand management. In *Proceedings of the 37th*  
459 *Annual Conference of Operations Research Society of New Zealand*, pages 55–63, 2002.
- 460 [19] R. L. Fares, J. P. Meyers, and M. E. Webber. A dynamic model-based estimate of the value of  
461 a vanadium redox flow battery for frequency regulation in Texas. *Applied Energy*, 113:189–198,  
462 2014.
- 463 [20] J. Feng, A. Brown, D. O'Brien, and D. J. Chmielewski. Smart grid coordination of a chemical  
464 processing plant. *Chemical Engineering Science*, 136:168 – 176, 2015. Control and Optimization of  
465 Smart Plant Operations.
- 466 [21] H. Hao, T. Middelkoop, P. Barooah, and S. Meyn. How demand response from commercial  
467 buildings will provide the regulation needs of the grid. In *50th Annual Allerton Conference on*  
468 *Communication, Control, and Computing*, pages 1908–1913, 2012.
- 469 [22] M. G. Ierapetritou, D. Wu, J. Vin, P. Sweeney, and M. Chigirinskiy. Cost Minimization in an  
470 Energy-Intensive Plant Using Mathematical Programming Approaches. *Industrial & Engineering*  
471 *Chemistry Research*, 41:5262–5277, 2002.
- 472 [23] M. H. Karwan and M. F. Kebulis. Operations planning with real time pricing of a primary input.  
473 *Computers and Operations Research*, 34(3):848–867, 2007.
- 474 [24] B. Kirby, M. O'Malley, O. Ma, P. Cappers, D. Corbus, S. Kiliccote, O. Onar, M. Starke, and  
475 D. Steinberg. Load Participation in Ancillary Services (Workshop Report). Technical Report  
476 December, U.S. Department of Energy, 2011.
- 477 [25] Y. Lin, P. Barooah, S. Meyn, and T. Middelkoop. Experimental Evaluation of Frequency Regula-  
478 tion From Commercial Building HVAC Systems. *IEEE Transactions on Smart Grid*, 6(2):776–783,  
479 2015.
- 480 [26] S. Meyn, P. Barooah, A. Busic, and J. Ehren. Ancillary service to the grid from deferrable loads:  
481 The case for intelligent pool pumps in florida. In *Decision and Control (CDC), 2013 IEEE 52nd*  
482 *Annual Conference on*, pages 6946–6953. IEEE, 2013.
- 483 [27] S. Mitra, I. E. Grossmann, J. M. Pinto, and N. Arora. Optimal production planning under time-  
484 sensitive electricity prices for continuous power-intensive processes. *Computers and Chemical*  
485 *Engineering*, 38:171–184, 2012.
- 486 [28] S. Mitra, L. Sun, and I. E. Grossmann. Optimal scheduling of industrial combined heat and  
487 power plants under time-sensitive electricity prices. *Energy*, 54:194–211, 2013.

- 488 [29] R. Mullin. CAISO regulation costs quadruple as prices, procurement jump, June 2016. RTO  
489 Insider.
- 490 [30] R. C. Pattison, C. R. Touretzky, T. Johansson, I. Harjunoski, and M. Baldea. Optimal process  
491 operations in fast-changing electricity markets: Framework for scheduling with low-order dy-  
492 namic models and an air separation application. *Industrial & Engineering Chemistry Research*,  
493 55(16):4562–4584, 2016.
- 494 [31] A. Rong and R. Lahdelma. Efficient algorithms for combined heat and power production  
495 planning under the deregulated electricity market. *European Journal of Operational Research*,  
496 176(2):1219–1245, 2007.
- 497 [32] D. Todd. They Said It Couldnt Be Done: Alcoas Experience in Demand Response. In *Texas*  
498 *Industrial Energy Management Forum: Energy Management in the Age of Shale Gas*, Houston, Texas,  
499 2013.
- 500 [33] D. Todd, M. Caufield, B. Helms, M. Starke, B. Kirby, and J. Kueck. Providing Reliability Services  
501 through Demand Response: A Preliminary Evaluation of the Demand Response Capabilities of  
502 Alcoa Inc. Technical report, Alcoa Power Generating, Inc; Oak Ridge National Laboratory, 2009.  
503 ORNL/TM-2008/233.
- 504 [34] R. Vujanic, S. Mariéthoz, P. Goulart, and M. Morari. Robust integer optimization and scheduling  
505 problems for large electricity consumers. In *American Control Conference (ACC), 2012*, pages 3108–  
506 3113. IEEE, 2012.
- 507 [35] R. A. Walling. Analysis of Wind Generation Impact on ERCOT Ancillary Services Requirements.  
508 Technical report, GE Energy, 2008.
- 509 [36] R. Wood and M. Berry. Terminal composition control of a binary distillation column. *Chemical*  
510 *Engineering Science*, 28(9):1707–1717, 1973.
- 511 [37] Q. Zhang, J. L. Cremer, I. E. Grossmann, A. Sundaramoorthy, and J. M. Pinto. Risk-based inte-  
512 grated production scheduling and electricity procurement for continuous power-intensive pro-  
513 cesses. *Computers & Chemical Engineering*, 86:90–105, 2016.
- 514 [38] Q. Zhang and I. E. Grossmann. Enterprise-wide optimization for industrial demand side man-  
515 agement: Fundamentals, advances, and perspectives. *Chemical Engineering Research and Design*,  
516 116:114–131, 2016.
- 517 [39] Q. Zhang, I. E. Grossmann, C. F. Heuberger, A. Sundaramoorthy, and J. M. Pinto. Air Separation  
518 with Cryogenic Energy Storage: Optimal Scheduling Considering Electric Energy and Reserve  
519 Markets. *AIChE Journal*, 61(5):1547–1558, 2015.
- 520 [40] Q. Zhang, M. F. Morari, I. E. Grossmann, A. Sundaramoorthy, and J. M. Pinto. An adjustable  
521 robust optimization approach to provision of interruptible load by continuous industrial pro-  
522 cesses. *Computers & Chemical Engineering*, 86:106–119, 2016.



- 523 [41] X. Zhang and G. Hug. Optimal regulation provision by aluminum smelters. In *2014 IEEE PES*  
524 *General Meeting — Conference Exposition*, pages 1–5, July 2014.
- 525 [42] X. Zhang and G. Hug. Bidding strategy in energy and spinning reserve markets for aluminum  
526 smelters’ demand response. In *2015 IEEE Power Energy Society Innovative Smart Grid Technologies*  
527 *Conference (ISGT)*, pages 1–5, Feb 2015.
- 528 [43] X. Zhang, G. Hug, Z. Kolter, and I. Harjunkoski. Industrial demand response by steel plants  
529 with spinning reserve provision. In *2015 North American Power Symposium (NAPS)*, pages 1–6,  
530 Oct 2015.
- 531 [44] P. Zhao, G. P. Henze, M. J. Brandemuehl, V. J. Cushing, and S. Plamp. Dynamic frequency reg-  
532 ulation resources of commercial buildings through combined building system resources using a  
533 supervisory control methodology. *Energy and Buildings*, 86:137–150, 2015.
- 534 [45] P. Zhao, G. P. Henze, S. Plamp, and V. J. Cushing. Evaluation of commercial building HVAC  
535 systems as frequency regulation providers. *Energy and Buildings*, 67:225–235, 2013.
- 536 [46] D. Zhou, K. Zhou, L. Zhu, J. Zhao, Z. Xu, Z. Shao, and X. Chen. Optimal scheduling of multi-  
537 ple sets of air separation units with frequent load-change operation. *Separation and Purification*  
538 *Technology*, 172:178 – 191, 2017.
- 539 [47] Y. Zhu, S. Legg, and C. D. Laird. A multiperiod nonlinear programming approach for operation  
540 of air separation plants with variable power pricing. *AIChE Journal*, 57(9):2421–2430, 2011.